





The antimicrobial activity of biogenic silver nanoparticles synthesized from extracts of Red and Green European pear cultivars

Sohail Simon^{a,b} , Nicole Remaliah Samantha Sibuyi^{a,b} , Adewale Oluwaseun Fadaka^{a,b} ,
Mervin Meyer^{a,b} , Abram Madimabe Madiehe^{a,b} and Marlene Geraldine du Preez^a

^aDepartment of Biotechnology, University of Western Cape, Cape Town, South Africa; ^bDepartment of Science and Innovation/Mintek Nanotechnology Innovation Centre (DSI/Mintek NIC), Biolabels Node, Department of Biotechnology, University of Western Cape, Cape Town, South Africa

ABSTRACT

Green nanotechnology stands amongst the leading giants of innovation for the twenty first century technological advances. More interesting, is the use of natural products as reducing agents. These could be recyclable materials from fruits and vegetables to produce nanoparticles (NPs) with novel properties. In the current study, silver NPs (AgNPs) were synthesized using the water extracts from the peel and flesh of two *Pyrus communis* L. cultivars, namely, the Forelle (Red) Pears (RPE) and Packham Triumph (Green) Pears (GPE). The AgNPs were characterized by UV-Vis spectrophotometry, Dynamic Light Scattering (DLS), High Resolution Transmission Electron Microscopy (HRTEM) and Fourier Transform Infra-Red Spectroscopy (FTIR). The antibacterial activities of the AgNPs were evaluated using agar well diffusion and microdilution assays. The cytotoxicity of the AgNPs was investigated on a rat macrophage (RAW 264.7) cells using MTT assay. Both the RPE and GPE were capable of synthesizing the AgNPs at high temperatures (70 and 100 °C). The AgNPs exhibited antibacterial activity against the test strains, and also had low toxicity towards the RAW 264.7 cells. Thus, the synthesized AgNPs have a potentially viable use in bio-applications for treatment of bacterial infections.

ARTICLE HISTORY

Received 23 February 2021
Revised 25 August 2021
Accepted 3 September 2021

KEYWORDS

Anthocyanins; antibacterial agents; Forelle Pears; green nanotechnology; nutraceuticals; Packham Triumph Pears; silver nanoparticles

Introduction

Green nanotechnology has brought a lot of exciting opportunities that could be beneficial to waste recycling in the agricultural sector [1,2]. A large volume of fruit and vegetable wastes are discarded daily. Since these waste products contain useful phytochemicals, they could instead be recycled to harness the bio-active compounds and incorporate them into new products [2,3]. The use of fruit, vegetable or plant extracts in the biological synthesis of nanoparticles (NPs) is an attractive approach as plant materials are readily available [4]. Plant extracts reported in the synthesis of NPs contain antioxidants such as phenolic acids and flavonoids [4,5], with valuable functional groups such as hydroxyl, carboxyl, carbonyl and phenol groups. These functional groups are involved in the reduction of various metals (silver, gold and palladium) into their respective metallic NPs [6].

Metallic NPs, such as silver nanoparticles (AgNPs) are of particular interest. These NPs exhibit a number of properties that are useful in food sciences [1,2], biosensors [2,7] nanobiotechnology, nanomedicine, textile, etc. The NPs at a size range of 1–100 nm [8,9] have been shown to have unique and novel properties [8]. Due to their unique physical and chemical properties, AgNPs are widely used in nanomedicine

as antimicrobial [3,10], as antiseptic agents in the clothing industry, as well as in the development of skincare products [11].

The current study explores the synthesis of AgNPs using the European pear or *Pyrus communis* L. This pear fruit is common in temperate zones worldwide, and has over 2000 variants [12,13]. The Packham's Triumph (Green) and Forelle (Red) are among pear variants available in South Africa [14]. The red-skinned appearance of Forelle pears is due to the high amounts of anthocyanins [15]. Anthocyanins are flavonoids that are responsible for the various colours in flowers, vegetables and fruits. They have been shown to have a number of properties, which include antibacterial, antioxidant, and anticancer bioactivities [16]. Anthocyanin-rich fruits, such as blackberry (*Rubus fruticosus* L.), strawberry (*Fragaria vesca* L.) and raspberry (*Rubus idaeus* L.), have been used to synthesize AgNPs with an antimicrobial activity using green nanotechnology [17].

The pear industry is the third-largest in the South African fruit industry after citrus and apples [18]. The *Pyrus* spp. is extremely nutritious and a rich source of phytochemicals associated with health benefits (nutraceuticals). These phytochemicals are excellent candidates for the synthesis of bio-active AgNPs [19,20]. While the synthesis of both gold NPs

CONTACT Marlene du Preez  mgdupreez@uwc.ac.za; Mervin Meyer  memeyer@uwc.ac.za 

© 2021 The Author(s). Published by Informa UK Limited, trading as Taylor & Francis Group
This is an Open Access article distributed under the terms of the Creative Commons Attribution License (<http://creativecommons.org/licenses/by/4.0/>), which permits unrestricted use, distribution, and reproduction in any medium, provided the original work is properly cited.

[21] and AgNPs [19,20,22] have been demonstrated using Asian pear variants, such as the Huangguan pear (*Pyrus bretschneideri* Rehder); the European pears have not been used previously to synthesize AgNPs. Both the appearance and phytochemical composition of the Asian and European pears differ significantly. Asian pear variants contain more glucose compared to European pears, which have higher fructose to glucose ratio and a higher concentration of sorbitol [23]. It is, therefore, possible that the characteristics of the AgNPs produced from the green and red European pear variants will be different. In this study, we demonstrate the synthesis of AgNPs from aqueous extracts of Packham's Triumph and Forelle pears and show their antibacterial activity against several bacterial strains.

Materials and methods

Preparation of the pear water extract

The Green (Packham Triumph) and the Red (Forelle) pears were a kind gift from Kromco (Pty) Ltd (Grabouw, South Africa). Five pears each from green and red pears were washed with distilled water (dH₂O) and dried with a paper towel. The peel and flesh were separated and individually blended in 400 mL boiled dH₂O. The crushed material was centrifuged at 9000 rpm for 30 min using the Sorval Lynx 6000 centrifuge (Thermo Fisher Scientific, USA). The supernatant was vacuum filtered using Whatman 0.45 µm filters (Merck, Germiston, South Africa). The filtrates were frozen at -80 °C and freeze-dried using a freeze dryer (Virtis, Gardiner, NY, USA). The extracts were dissolved in dH₂O to obtain Green and Red Pear Peel (GPP and RPP, respectively) and Pear Flesh (GPF and RPF, respectively) extracts.

Phytochemical analysis of the pear-extracts

The Total Phenolic Content (TPC) analysis was evaluated in the RPE and GPE following the Folin-Ciocalteu assay using 0–1 mg/mL gallic acid (Sigma, St. Louis, USA) as a standard, following a previously described protocol [24]. The TPC was expressed as µg/mL equivalents of gallic acid.

The reducing sugars in the RPE and GPE were analysed following the phenol-sulfuric acid reaction method using 0–25 mg/mL D-glucose (Sigma) solution as a standard, following a previously described protocol [25].

Synthesis of AgNPs

Synthesis of AgNPs was performed by reducing AgNO₃ (Sigma, St. Louis, MO, USA) with the GPE and RPE. The AgNPs were synthesised by mixing the pear extracts and AgNO₃ solution in a 1:3 (v/v) ratio (i.e. 0.5 mL extract: 1.5 mL AgNO₃). Synthesis was performed using different concentrations of the extracts (1.563–50 mg/mL), AgNO₃ solution (0.5, 1, 2 and 3 mM), temperatures (25, 70 and 100 °C), and pH ranges (4, 5, 6, 7, 8, 9 and 10). All the reactions were incubated for 16 h at their set conditions, with shaking. After the incubation period, all the samples were inspected for a colour change

and imaged using a digital camera. The reactions were performed in 2 mL tubes in an Eppendorf Thermomixer Comfort (Hamburg, Germany) while shaking at 400 rpm.

Characterization of the AgNPs

The AgNPs were centrifuged using an Eppendorf centrifuge 5417 R (Hamburg, Germany) at 14,000 rpm for 10 min to remove unreacted extract and AgNO₃ before analysis. The AgNPs were characterized by UV-Vis using a POLARstar Omega Plate reader (BMG Labtech, Offenburg, Germany) at a wavelength ranging from 300 to 700 nm, Dynamic Light Scattering (DLS) using a Malvern NanoZS90 Zetasizer (Malvern Panalytical Ltd., Enigma Business Park, UK), FTIR spectra read on an FTIR spectrophotometer (Perkin Elmer, Waltham, MA, USA) in a 500–4000 cm⁻¹ wavenumber range, and HRTEM using Tecnai F20 Field Transmission Electron Microscope (FEI Company, Oregon, USA), as previously described [26].

Bioactivity of the AgNPs

Antibacterial activity of the AgNPs

Staphylococcus aureus, MRSA, *Pseudomonas aeruginosa*, and *Escherichia coli* were used to assess the antibacterial activity of the pear extracts and AgNPs. The bacterial strains were purchased from American Tissue Culture Collection (ATCC; Manassas, VA, USA). The bacterial cultures were adjusted to 0.5 McFarland standard at OD_{600nm} between 0.08 and 0.1. The cultures were then diluted to 1:150 with fresh Müller Hinton Broth (MHB, Sigma), and used for agar well diffusion and microdilution assays, as previously described [5,26].

Agar well diffusion assay

Microorganisms were streaked on the Müller Hinton Agar (MHA, Sigma) plates. Then 50 µL each of the negative control (MHB), positive control (1:1 penicillin-streptomycin (Pen-Strep) cocktail at 10 U/mL) (Gibco, Bleiswijk, The Netherlands), pear extracts and the AgNPs were added in triplicates into their respective wells.

Determination of minimum inhibitory concentration (MIC)

The microorganisms were exposed to the pear extracts and AgNPs at concentrations of 0 to 500 µg/mL, for 24 h. The MIC was recorded for each treatment, and the OD_{600nm} was measured for each treatment using the POLARstar Omega Plate reader.

Evaluation of the cytotoxicity of the AgNPs

Cytotoxicity of the pear extracts and AgNPs was evaluated in RAW 264.7 cells (ATCC) using the 3-(4,5-dimethylthiazol-2-yl)-2,5-diphenyltetrazolium bromide (MTT, Sigma) assay, as previously described [27]. The cells were grown in Dulbecco's Modified Eagles Medium (Gibco, Roche, Germany) supplemented with 10% foetal bovine serum (Gibco) and 1% Pen-Strep. The cells were treated with 0–500 µg/mL pear

Table 1. Analysis of TPC and reducing sugars in the pear-extracts.

Pear extracts	TPC ($\mu\text{g/mL}$)	Reducing sugars ($\mu\text{g/mL}$)
RPP	16	75
RPF	38	45
GPP	127	51
GPF	65	36

extracts and AgNPs. Doxorubicin (Sigma) at a concentration of 50 $\mu\text{g/mL}$ was used as a positive control.

Statistical analysis

The data are expressed as mean \pm standard error of the mean of three independent experiments, with each condition performed in triplicate. Statistical analysis was performed by two-way ANOVA using GraphpadTM Prism v6 software, and *t*-test using Microsoft Excel (2010). The differences between the samples were considered statistically significant when the $p < .05$.

Results and discussion

Green synthesis of AgNPs

Green nanotechnology provides safer, inexpensive, and eco-friendly methods for the synthesis of NPs using natural products as reducing, capping and stabilizing agents [5,26]. These green chemistry principles-based methods replace the toxic reducing agents that are used in chemical synthesis methods. The natural products derived from either microorganisms or plants can be biomolecules and/or secondary metabolites that have the ability to reduce metal precursors into metallic NPs [28,29]. In recent years, green nanotechnology has shifted interest to the use of food wastes, including, fruits and vegetables for the synthesis of NPs. These waste products were shown to produce bio-active NPs [3,30–32] that are biocompatible and have selective toxicity [31].

Pears have high quantities of nutraceuticals, such as phenolic acid, flavonoids, and triterpenes. The phenolic acids include gallic acid, ferulic acid, ursolic acid, etc. [13,33]. Similar phenolic acids have been implicated in the green synthesis of NPs [31,34,35]. The nutraceuticals certainly vary among the pear variants [13,33]. As shown in Table 1, the RPE (both the peel and flesh) had a higher reducing sugar content and lower TPC compared to the GPE. The phenolic compounds are the major phytochemicals in plant extracts and prospective reducing agents in the green synthesis of metallic NPs [36–38], while the sugars can be used as reducing and/or stabilizing agents [39]. Their presence in the pear extracts substantiates their role in the reduction of AgNO_3 and stabilization of the AgNPs.

Synthesis of NPs can be influenced by many factors, such as temperature, pH, and concentrations of extract and AgNO_3 . Variations of these parameters can alter the size, shape, reaction rate, and activity of the NPs [26,40]. The effects of these parameters were investigated in this study.

Effect of extract concentration and temperature on AgNP synthesis

To determine the optimal extract concentration and temperature for the synthesis of AgNPs, various concentrations of RPE and GPE were incubated with 1 mM AgNO_3 . Changes in colour from clear to yellow and then brown indicated successful synthesis of the AgNPs, and were further confirmed by UV-Vis analysis (Figure 1). As shown in Figure 1(A), there was no colour change in the samples that were incubated at room temperature ($\sim 25^\circ\text{C}$) for all concentrations. This was further confirmed by UV-Vis spectra of these samples, indicating the absence of the characteristic peak around 400–500 nm, thus further indicating that there was no formation of RP-AgNPs at 25°C . These variable effects of temperature have been reported previously and attributed to the different types of phytochemicals in a particular plant extract. While the *Acinetobacter calcoaceticus* extracts were unable to synthesise AgNPs at 20°C [40], the extracts from *Salvia africana-lutea*, *Sutherlandia frutescens* [26] and *Terminalia Mantaly* [5] produced AgNPs at 25°C .

RPE-synthesized AgNPs were visible from 6.25 to 50 mg/mL at 70°C (Figure 1(B)), and in all tested concentrations for reactions at 100°C (Figure 1(C)). The corresponding UV-Vis spectra showed surface plasmon resonance (SPR) peaks around 400–450 nm. SPR is defined as a phenomenon where the electrons of the metal involved in the NP synthesis (Ag in this case) become excited by the photons at a certain angle of incidence [41]. AgNPs display a characteristic SPR peak around 400–450 nm [5,26,42]; which is also used to profile NP size, shape, stability, and estimate NP concentration [43].

Similar effects of temperature and extract concentrations were observed for GP-AgNPs, as shown in Figure 2. At 25°C , there was no colour change or UV-Vis spectra in all the GPE- AgNO_3 reactions. Colour changes to light yellow, orange and brown were observed at 70°C and 100°C . This was demonstrated by the absence or presence of the SPR peaks in the UV-Vis spectra around 400–450 nm. In essence, the colour change and presence of SPR suggested the formation of AgNPs [5,26,44].

The intensity of the colour, as well as the absorbance, are directly proportional to the production rate and the concentration of the NPs [26,43,45]. These two parameters were used in the selection of the optimum pear extract concentration and temperature. The 100°C was the optimal temperature for the synthesis of the RP-AgNPs and GP-AgNPs. At this temperature, all the RPE and GPE concentrations produced AgNPs with more intense colours than at 70°C . Moreover, the AgNPs at 70°C produced broader UV-Vis peaks compared to 100°C , signifying the production of polydispersed AgNPs at 70°C . Based on these parameters, the optimum concentrations of the pear extracts were 3.125 mg/mL for the peel extract and 6.25 mg/mL for the flesh extract.

Effect of pH on AgNP synthesis

A yellow to brown colors were observed at all pH conditions, confirming the synthesis of the AgNPs. As shown in Figure 3,

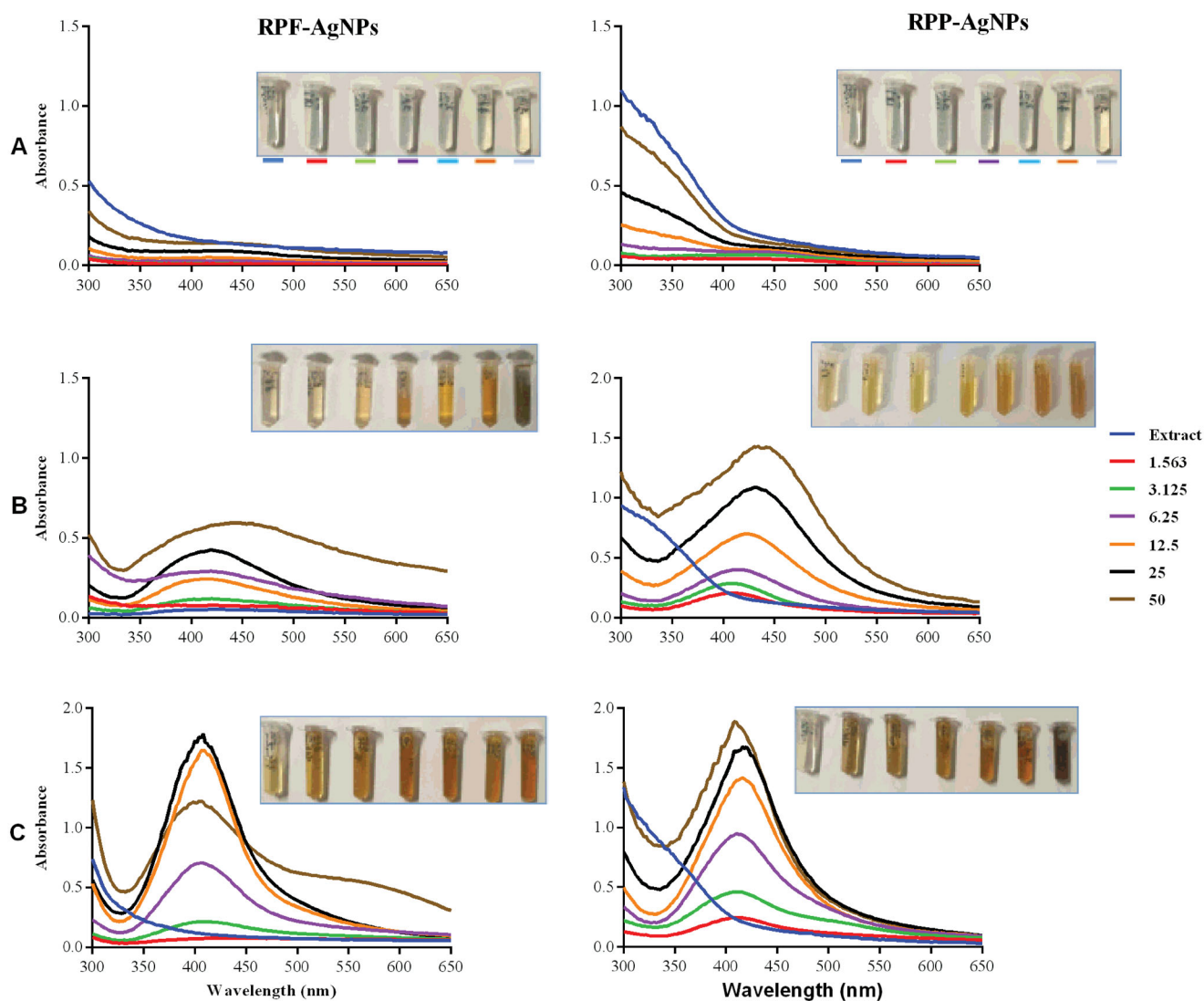


Figure 1. Effect of temperature and concentration of RPE on the synthesis of RP-AgNPs. The RP-AgNPs were synthesized at 25 °C (A), 70 °C (B), and 100 °C (C).

the peel extracts produced narrow UV-Vis spectra (A and C), while the flesh produced broad spectra (B and D). This further indicates that the peel extracts at high pH synthesize AgNPs that have a narrow size distribution and uniform shapes, whereas, the low pH conditions synthesized larger AgNPs that are likely to be polydispersed. The pH of the samples is often adjusted to control NP sizes and reaction rate. AgNPs synthesized at low pH aggregate over time and have a wide range of shapes and sizes. On the other hand, AgNPs synthesized at high pH are smaller in size and have uniform shapes [43,46]. Using *Lawsonia inermis* leaf extracts, AgNPs could only be synthesized at pH 9 and not at pH 4 [46]. *Parachlorella kessleri* synthesized smaller AgNPs with a core size range of 10–25 nm at pH 10 and larger AgNPs (10–60 nm core size) at pH 4 [43]. Similarly, ascorbic acid and citrate-reduced AgNPs were smaller with uniform shapes at high pH [47]. Based on the results for all pear extracts, pH 10 appeared to be the optimum pH for AgNP synthesis. The UV-Vis spectra for the AgNPs at their native pH (pH 4 for the RPE and GPF extracts, pH 5 for the GPP extracts) were broad

and had a low SPR which directly corresponds to non-uniform AgNP shapes and low concentration, respectively [40].

Effect of AgNO₃ concentration on AgNP synthesis

The concentration of the metal precursor also plays a crucial role in the synthesis of metallic NPs [40]. Some studies reported a positive correlation between the precursor concentration and the amount of NPs formed. By increasing the concentration of AgNO₃ the rate of *Gum tragacanth* AgNPs formation was increased [45]. Contrary, more AgNPs were synthesised from *Acinetobacter calcoaceticus* extracts at low (0.5 and 0.7 mM) than at higher (5 mM) AgNO₃ concentrations. Moreover, lower concentrations of AgNO₃ were associated with smaller and uniform AgNPs compared to higher concentrations [40]. A positive correlation between the concentration of AgNO₃ and AgNPs formation was observed in Figure 4. Although the SPR in the GPF-AgNPs was not as profound when compared to the SPR of the other AgNPs (Figure 4(D)), it was apparent that AgNPs were present and was

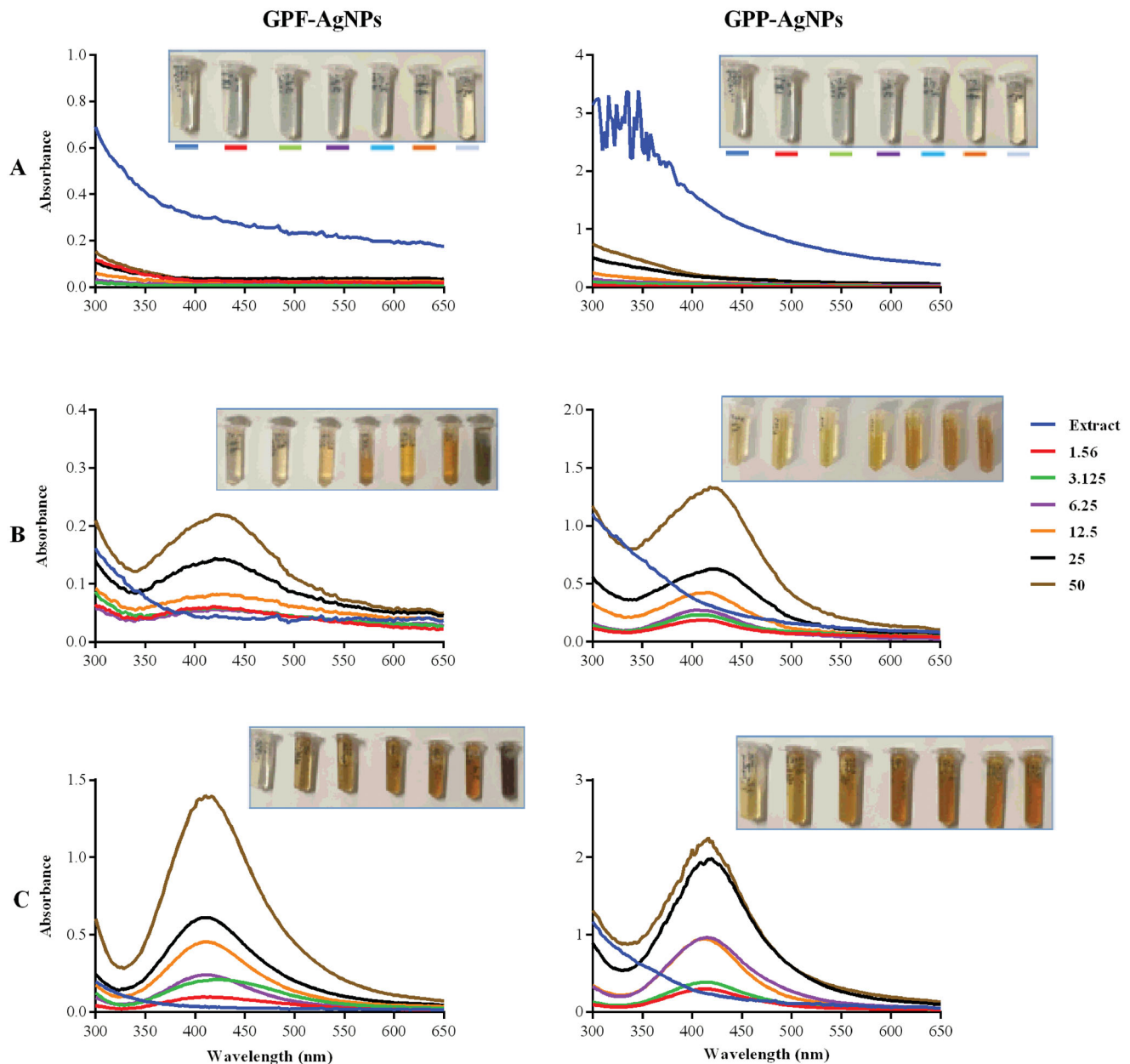


Figure 2. Effect of temperature and concentration of GPE on the synthesis of GP-AgNPs. The GP-AgNPs were synthesized at 25 °C (A), 70 °C (B), and 100 °C (C).

supported by the color change. The optimum AgNO_3 concentration for the synthesis of the AgNPs was determined as 1 mM.

Synthesis and characterization of optimized AgNPs

The AgNPs were then synthesized using the optimum conditions, that is, 3.125–6.25 mg/mL extract concentration, pH 10, 1 mM AgNO_3 , and 100 °C. Figure 5(A) shows the UV-Vis spectra of the RP-AgNPs and GP-AgNPs with their SPR peaks at 408–432 nm. The SPR of the AgNPs is indicated in Table 2. There was a red-shift in the SPR of the RP-AgNPs (432 nm for RPP-AgNPs and 424 nm for RPF-AgNPs) and a blue-shift for the GP-AgNPs (408 nm for GPP-AgNPs, 416 nm for GPF-AgNPs). The absorbance of GPP-AgNPs and RPP-AgNPs at SPR was higher than that of GPF-AgNPs and RPF-AgNPs,

which indicated that the concentration of the AgNPs synthesized from the peel extracts was higher than AgNPs from the flesh extracts [42].

The majority of the AgNPs were spherical in shape and had varying core size distributions, as indicated by HRTEM images (Figure 5(B,C)). The RPE produced AgNPs with larger core sizes than the GPE. The core size distribution of the RPE-AgNPs was in the size range of 10–70 nm, with the average core size of 43 nm and 46 nm for RPP-AgNPs and RPF-AgNPs, respectively (Table 2). The core size distributions of the GPE-AgNPs were at 5–40 nm range, with an average core size of 20 nm and 25 nm for GPP-AgNPs and GPF-AgNPs, respectively. The hydrodynamic size distribution of the AgNPs determined by DLS showed larger sizes. (Figure 5(D)). The Z (d.nm) average of the peel AgNPs was smaller than that of the flesh AgNPs (Table 2). These sizes were different from the core size obtained from the HRTEM images (Figure 5(B)). This

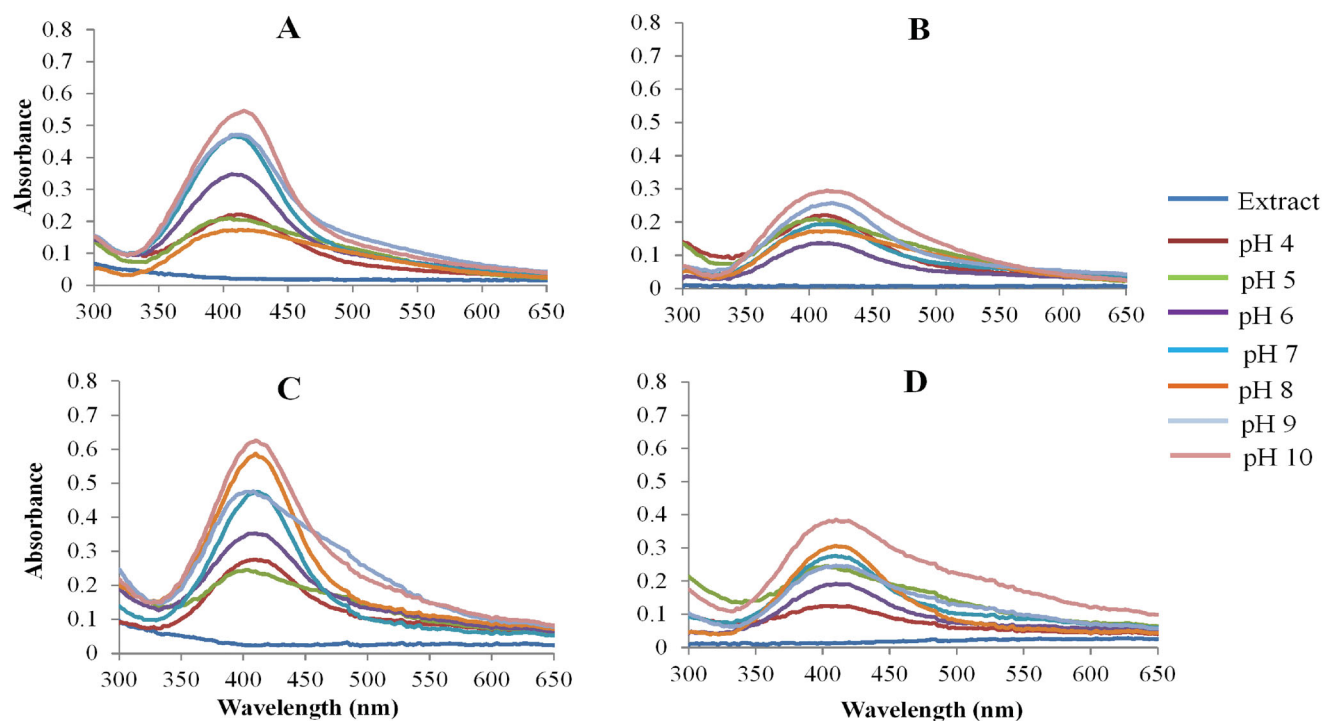


Figure 3. Effect of pH on the synthesis of AgNPs. UV-Vis spectra of RPP-AgNPs (A), RPF-AgNPs (B), GPP-AgNPs (C) and GPF-AgNPs (D) at 100 °C.

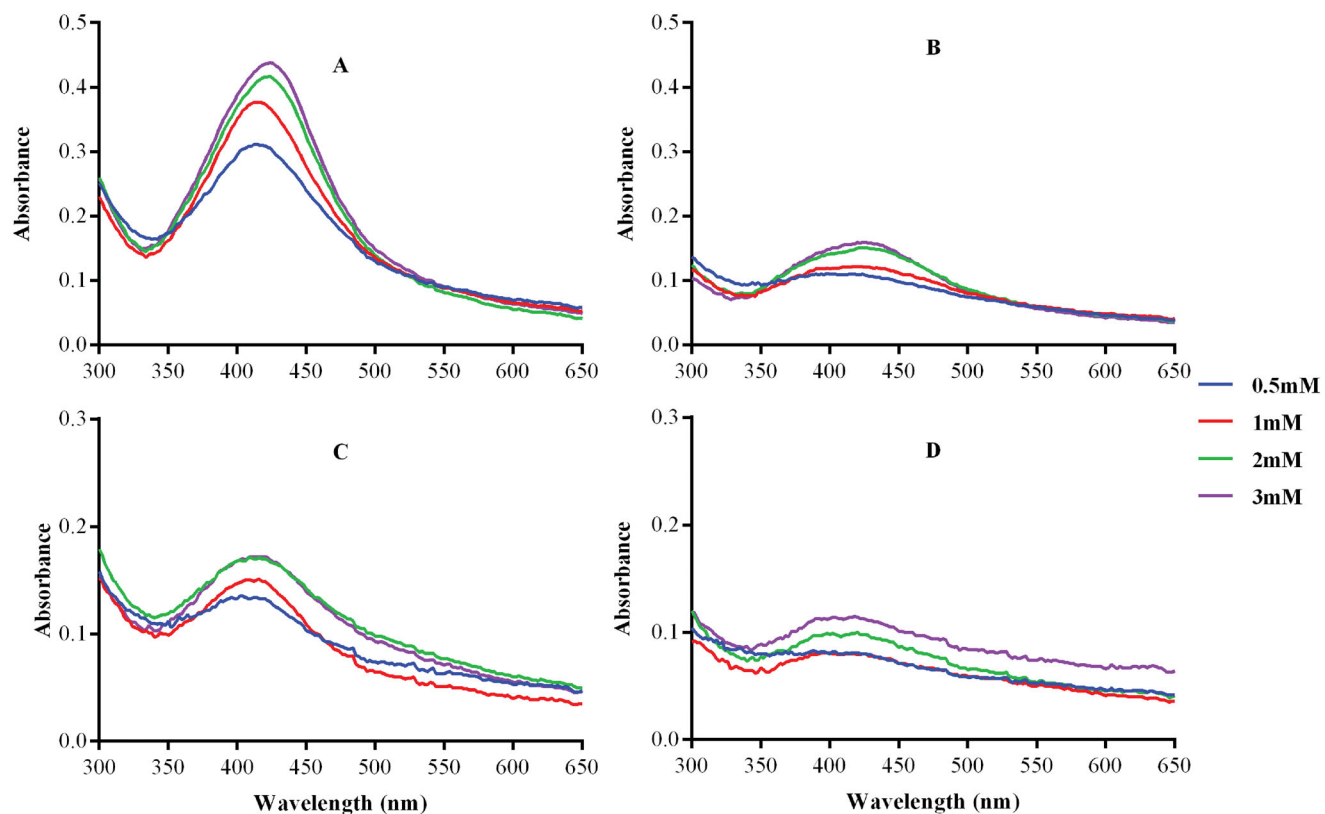


Figure 4. Effect of AgNO_3 concentrations on the synthesis of AgNPs. The AgNPs were synthesized at optimal pear extract concentrations, temperature and different concentrations of AgNO_3 . The UV-Vis spectra represent (A) RPP-AgNPs, (B) RPF-AgNPs, (C) GPP-AgNPs and (D) GPF-AgNPs at 100 °C.

is due to the fact that the hydrodynamic diameter of the AgNPs was augmented by the phytochemicals on the surface of the AgNPs [5,26], which made their average hydrodynamic size much higher than that of the metal core size [5,26,48]. The size difference in the core and hydrodynamic diameters

could be attributed to the content of phytochemical components in the pear extracts. Phenolic acids and flavonoids occur in different combinations and concentrations and can influence the size of the AgNPs. This is supported by Krishnaraj et al. who synthesized AgNPs in the size range of

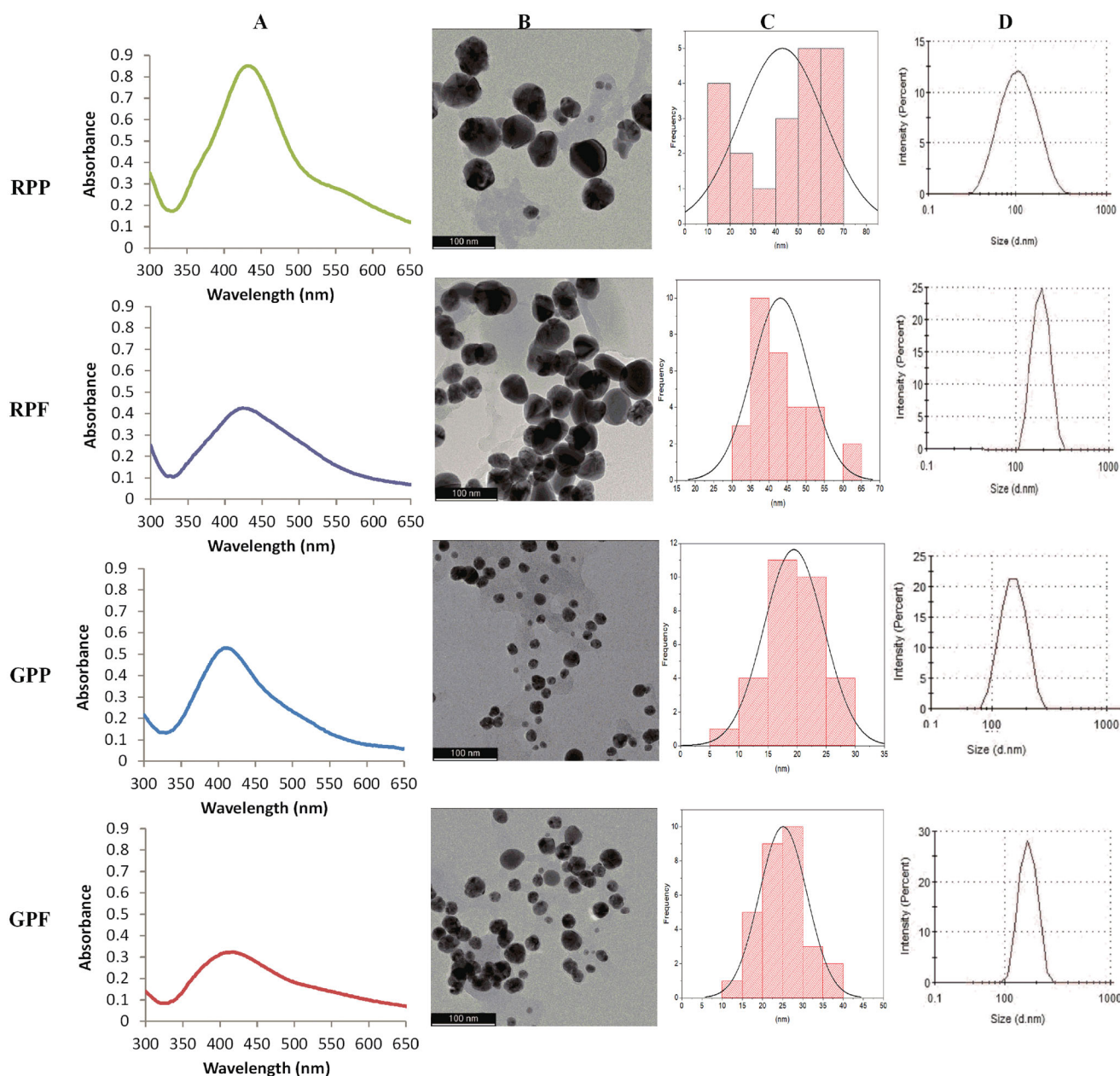


Figure 5. Physico-chemical properties of the AgNPs at the optimal conditions. The AgNPs were characterized by UV-Vis (A), HRTEM (B) and DLS (D). The core size of the AgNPs was calculated from the HRTEM images by ImageJ software (C).

Table 2. The physico-chemical properties of the optimized GP-NPs and RP-NPs.

AgNPs	UV-Vis analysis			HRTEM analysis	DLS analysis		
	[Extract] mg/mL	SPR (nm)	Absorbance at SPR	Core size distribution (nm)	Z average (d nm)	Pdi	ζ -potential (mV)
RPP-AgNPs	3.125	432	0.852	10–70	117.2	0.244	−9.5
RPF-AgNPs	6.25	424	0.425	30–65	190	0.460	−1.1
GPP-AgNPs	3.125	408	0.529	10–40	157.1	0.383	−7.7
GPF-AgNPs	6.25	416	0.324	5–30	168.1	0.545	−3.4

20–30 nm using *Acalyphia indica* plant extracts [49], whereas Banala et al. synthesized AgNPs in the size range of 5–50 nm using *Carica papaya* leaf extracts [50].

The Pdi of the AgNPs was below 0.6 (Table 2). This also supports the TEM and DLS data that showed that their size distribution range was not too broad. All the AgNPs had negatively charged ζ -potential values (Table 2), thus

indicating strong repulsive forces between the AgNPs which will prevent aggregation of AgNPs in solution [48].

FTIR analysis of optimized AgNPs

The FTIR analysis of the pear extracts and AgNPs in Figure 6 shows that the extracts contain the same functional groups

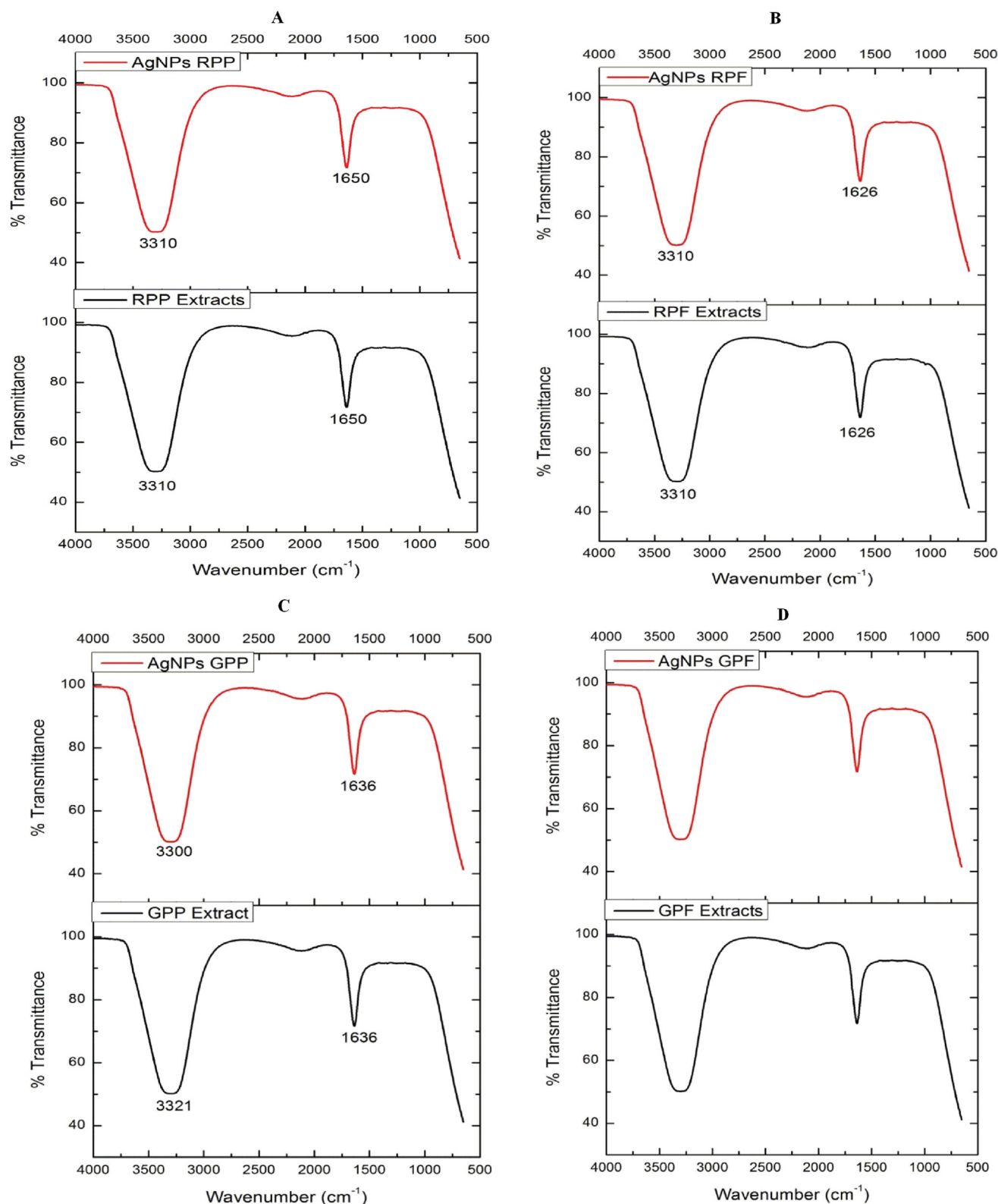


Figure 6. Comparison of the FTIR spectra of the pear extracts and AgNPs. FTIR of RPP-AgNPs versus RPP (A), RPF-AgNPs versus RPF (B), GPP-AgNPs versus GPP (C), GPF-AgNPs versus GPF (D). Each peak in the AgNPs indicates the functional group of the phytochemical involved in the NP synthesis.

as those in their respective AgNPs. This indicated that the functional groups present in the pear extracts played a role in the reduction of AgNO_3 , and stabilization of the AgNPs [51]. Two prominent absorption peaks were observed at ~ 1650 and 3300 cm^{-1} . The peaks at $\sim 1650\text{ cm}^{-1}$ represent

the involvement of an amide-bond (NH-C=O) which might probably come from proteins [52]. The peaks at $\sim 3300\text{ cm}^{-1}$ suggest the presence of hydroxyl or amine groups, which could indicate the interaction between the silver ions (Ag^+) and hydroxyl or amine groups of the RPE and GPE. These

functional groups are among the ones identified in the AgNPs synthesized from the Huangguan pear juice extracts [20], which could be equivalent to the AgNPs synthesized using RPF and GPF extracts. This further implies that proteins, in addition to the reducing sugars and phenolic compounds, found in pear extracts were involved in the synthesis of the AgNPs.

Antibacterial effects of AgNPs

The antibacterial effects of the AgNPs were investigated using agar well diffusion against two Gram-positive (*S. aureus*, MRSA) and two Gram-negative (*E. coli* and *P. aeruginosa*)

Table 3. ZOI for bacteria treated with the AgNPs.

Bacterial strains	Zones of inhibition (mm)				
	Pen-Strep	GPP-AgNPs	GPF-AgNPs	RPP-AgNPs	RPF-AgNPs
<i>E. coli</i>	8	1.8	3.0	2.5	4.1
<i>S. aureus</i>	6	1.5	3.5	2.9	4.0
<i>P. aeruginosa</i>	9	2.2	3.1	3.0	4.3
MRSA	5	1.3	2.8	2.3	3.7

bacterial strains. The presence of ZOI was used as a sign of bacterial growth inhibition. The RPE and GPE had no activity on the four strains (data not shown), while they were susceptible to the effects of Pen-Strep, which was used as the positive control. Pen-Strep is a cocktail of two commercial antibiotics, penicillin and streptomycin with well-known antimicrobial activity [53]. AgNPs synthesized from the pear flesh showed higher antibacterial activity than the AgNPs synthesized from the pear peels. As shown in Table 3, the AgNPs synthesized from the Forelle pear extracts (RP-AgNPs) had enhanced antibacterial activity when compared to the AgNPs synthesized from the Packham's Triumph pear extracts (GP-AgNPs). Huang et al. also demonstrated that AgNPs synthesized from the juice of the Asian Huangguan pear inhibit the growth of *P. aeruginosa*, *E. coli* and *S. aureus* [20]. Huang et al. further demonstrated that the ZOIs were size-dependent and larger than AgNPs produced by citrate reduction [20].

The MICs, lowest concentrations of the samples that inhibited visual growth of the bacteria are recorded in Table 4. The pear extracts showed no effect on bacterial growth. The GPF-AgNPs were the most active among the AgNPs. This was

Table 4. Evaluation of the MICs for the pear extracts and AgNPs.

Bacterial strains	MIC ($\mu\text{g/mL}$)							
	GPP	GPP-AgNPs	GPF	GPF-AgNPs	RPP	RPP-AgNPs	RPF	RPF-AgNPs
<i>E. coli</i>	>500	>500	>500	500	>500	>500	>500	>500
<i>S. aureus</i>	>500	>500	>500	500	>500	>500	>500	>500
<i>P. aeruginosa</i>	>500	500	>500	500	>500	500	>500	500
MRSA	>500	>500	>500	500	>500	>500	>500	>500

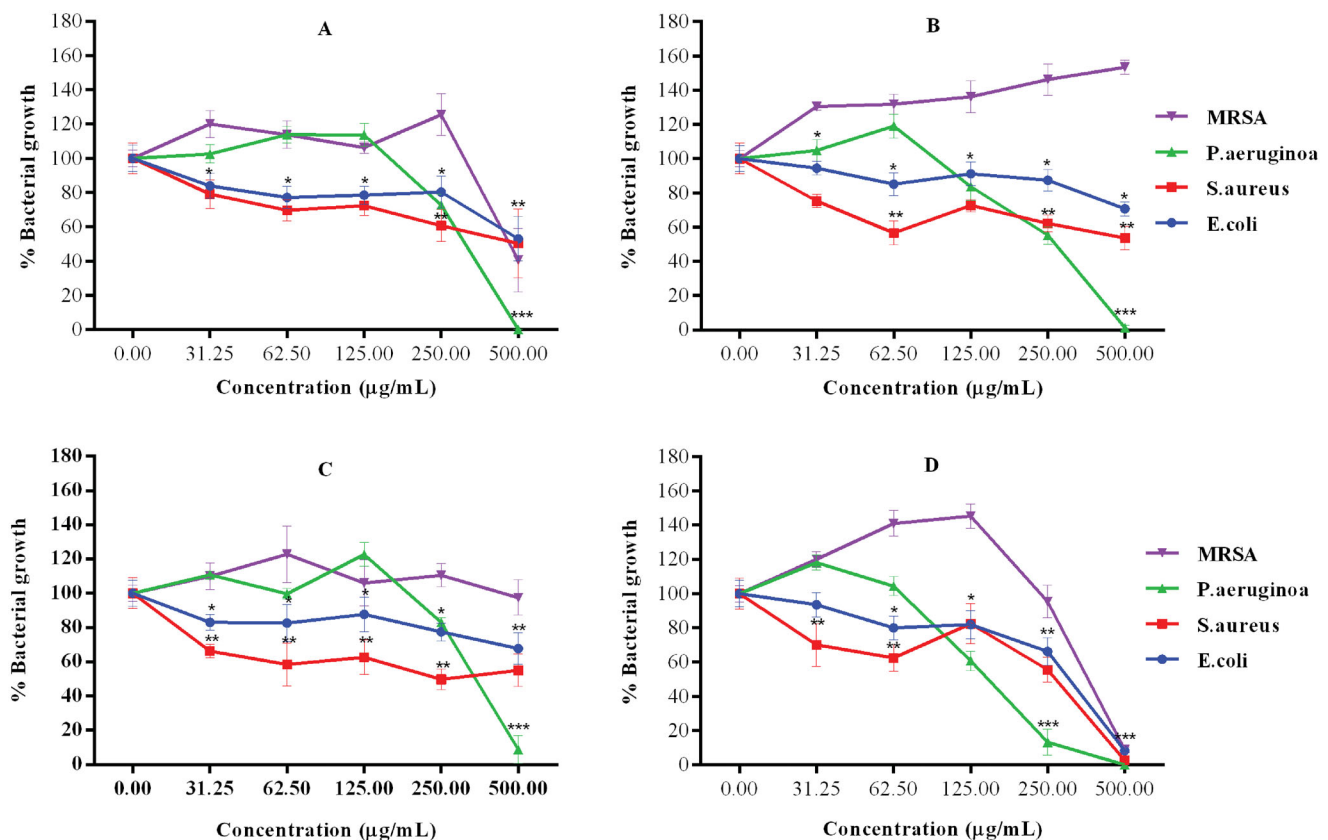


Figure 7. Growth inhibitory effects of the AgNPs against the selected bacterial strains. (A) RPP-AgNPs (B) RPF-AgNPs, (C) GPP-AgNPs and (D) GPF-AgNPs. *Statistically significant at $p < .05$, ** $p < .001$ and $p < .0001$.

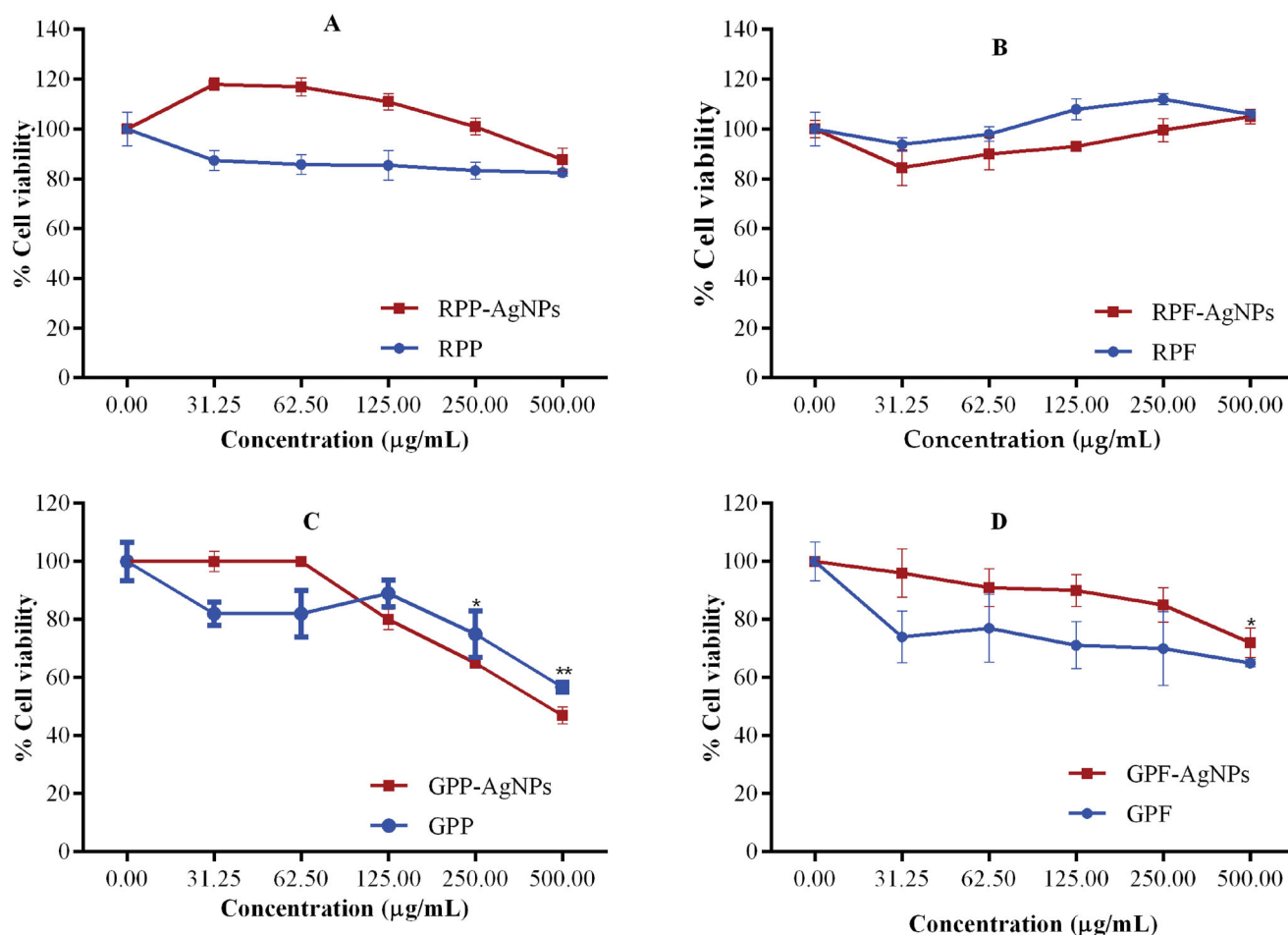


Figure 8. Cytotoxicity effects of the GP-AgNPs and RP-AgNPs on RAW 264.7 cells. Cell viability was assessed by MTT assay after 24 h exposure to increasing concentrations (0–500 µg/mL) of the RP-AgNPs (A, B) and the GP-AgNPs (C, D). *Statistically significant at $p < .05$, and ** $p < .001$.

based on the findings that these AgNPs inhibited visible growth for all the bacteria at 500 µg/mL. Of the four strains, *P. aeruginosa* was the only strain that was susceptible to all the AgNPs (Table 4). The antibacterial effects of the test samples were further confirmed by measuring the optical density of the treated bacteria at 600 nm (Figure 7). MRSA was most resistant to the effects of the AgNPs, especially the RPF-AgNPs and GPP-AgNPs which did not affect their growth rates, even at higher concentrations. *S. aureus*, *E. coli*, and to a lesser extent *P. aeruginosa*, showed susceptibility to the AgNPs in a dose-dependent manner. Growth of *P. aeruginosa* was completely inhibited by all the AgNPs at 500 µg/mL. This represents the minimum bactericidal concentration (MBC, lowest concentration that inhibits bacterial growth) of the AgNPs on *P. aeruginosa*. The antibacterial effects were statistically significant from 31.25 µg/mL for *E. coli* and *S. aureus*, and from 250 µg/mL for the other bacterial strains. Overall, the antibacterial effects of the RP and GP AgNPs followed similar trends in all the bacterial strains, except for MRSA. The RPP-AgNPs and the GPF-AgNPs are the only AgNPs that were effective against MRSA. The observed differential antibacterial effects could be due to the differences in the phytochemical composition in the RPE and GPE. However, while the main difference in the two pear variants is that RPE has a higher concentration of anthocyanins than GPE [15], it is

unlikely that anthocyanins are the only phytochemicals playing a role in the antibacterial activity of these AgNPs.

Cytotoxicity of AgNPs

The biocompatibility of the AgNPs was evaluated in RAW 264.7 cells using the MTT assay. The assay is used to quantifying the percentage of metabolically active cells by measuring mitochondrial enzymatic activities. Only viable cells are able to process the yellow MTT dye to produce an insoluble formazan product, which can be solubilized by the addition of DMSO to produce a purple colour that is proportional to the number of live cells [54]. The anthocyanin-rich RP extracts and AgNPs were less toxic to the cells when compared to GP extracts and AgNPs (Figure 8). The RPP and GPF extracts showed negligible toxicity towards the cells (Figure 8(A,D)). In contrast, their respective AgNPs seemed to offer protection to the cells. Significant toxicity was only observed in GPP extracts and AgNPs at concentration ≥ 250 µg/mL.

Conclusion

This study demonstrated the successful green synthesis of AgNPs using the aqueous peel and flesh extracts of the Packham's Triumph and Forelle pear variants. The method of

synthesis used was rapid, cost-effective, and eco-friendly. The GPF and RPP AgNPs exhibited significant antimicrobial activities against the multi-drug-resistant strains, that is, MRSA and *P. aeruginosa*. The synthesized AgNPs showed differential effects on the proliferation of RAW 264.7 cells, where the RP-AgNPs were biocompatible and less toxic compared to the GP-AgNPs. Thus, the synthesized AgNPs have a potential for use in bio-applications, such as skincare therapeutics, cosmetics, and the food industry to prevent spoilage. However, the safety of these AgNPs warrants further investigations for their use.

Acknowledgements

All authors herein are grateful for the research support by Mr. John Marais (Packhouse Quality Manager at Kromco [Pty] Ltd., Elgin, South Africa) who provided the Packham Triumph and the Forelle pears used in the study. The FTIR analysis was performed at the School of Pharmacy (UWC).





Disclosure statement

No potential conflict of interest was reported by the author(s).

Funding

This work was supported by the UWC, National Research Foundation and the DSI/Mintek NIC Biolabels Node.

ORCID

Sohail Simon  <http://orcid.org/0000-0002-6613-7726>
 Nicole Remaliah Samantha Sibuyi  <http://orcid.org/0000-0001-7175-5388>
 Adewale Oluwaseun Fadaka  <http://orcid.org/0000-0002-3952-2098>
 Mervin Meyer  <http://orcid.org/0000-0002-8296-4860>

Data availability statement

The data for the study is presented in the paper as figures and tables.

References

- He X, Deng H, Min Hwang H. The current application of nanotechnology in food and agriculture. *J Food Drug Anal.* 2019;27(1): 1–21.
- Ganachari SV, Yaradoddi JS, Somappa SB, et al. Green nanotechnology for biomedical, food, and agricultural application. In: *Handbook of ecomaterials*. New York (NY): Springer International Publishing; 2019. p. 2681–2698.
- Jabir MS, Saleh YM, Sulaiman GM, et al. Green synthesis of silver nanoparticles using *Annona muricata* extract as an inducer of apoptosis in cancer cells and inhibitor for NLRP3 inflammasome via enhanced autophagy. *Nanomaterials.* 2021;11:384.
- Ismail E, Khenfouch M, Dhlamini M, et al. Green palladium and palladium oxide nanoparticles synthesized via *Aspalathus linearis* natural extract. *J Alloys Compd.* 2017;695:3632–3638.
- Majoumou MS, Sibuyi NRS, Tincho MB, et al. Enhanced anti-bacterial activity of biogenic silver nanoparticles synthesized from *Terminalia mantaly* extracts. *Int J Nanomedicine.* 2019;14: 9031–9046.
- Zhao P, Li N, Astruc D. State of the art in gold nanoparticle synthesis. *Coord Chem Rev.* 2013;257(3–4):638–665.
- Nasrollahzadeh M, Sajadi SM, Sajjadi M, et al. Applications of nanotechnology in daily life. In: *Interface science and technology*. Amsterdam (The Netherlands): Elsevier; 2019. p. 113–143.
- Dubey SP, Lahtinen M, Sillanpää M. Green synthesis and characterizations of silver and gold nanoparticles using leaf extract of *Rosa rugosa*. *Colloids Surfaces A Physicochem Eng Asp.* 2010; 364(1–3):34–41.
- Hussain I, Singh NB, Singh A, et al. Green synthesis of nanoparticles and its potential application. *Biotechnol Lett.* 2016;38(4): 545–560.
- Sulaiman GM, Ali H, Jabbar II, et al. Synthesis, characterization, antibacterial and cytotoxic effects of silver nanoparticles. *Dig J Nanomater Biostructures.* 2014;9:787–796.
- Gurunathan S. Rapid biological synthesis of silver nanoparticles and their enhanced antibacterial effects against *Escherichia fergusonii* and *Streptococcus mutans*. *Arab J Chem.* 2019;12(2):168–180.
- Raffo MD, Ponce NMA, Sozzi GO, et al. Compositional changes in ‘Bartlett’ pear (*Pyrus communis* L.) cell wall polysaccharides as affected by sunlight conditions. *J Agric Food Chem.* 2011;59(22): 12155–12162.
- Kolniatek J, Kłopotowska D, Rutkowski KP, et al. Bioactive compounds and health-promoting properties of pear (*Pyrus communis* L.) fruits. *Molecules.* 2020;25:4444.
- Ferrandi CH, Van Der Merwe PW, Huysamer M. Status of the pear industry in Africa, with specific reference to South Africa. *Acta Hort.* 2005;671:73–76.
- Pierantoni L, Dondini L, Musacchi S, et al. Gene expression patterns underlying red skin colour in “max red bartlett” (PYRUS COMMUNIS), a “Williams” bud mutation. *Acta Hort.* 2009;814: 567–570.
- Abbasi BH, Nazir M, Muhammad W, et al. A comparative evaluation of the antiproliferative activity against HepG2 liver carcinoma cells of plant-derived silver nanoparticles from basil extracts with contrasting anthocyanin contents. *Biomolecules.* 2019;9:320.
- Demirbas A, Yilmaz V, Ildiz N, et al. Anthocyanins-rich berry extracts directed formation of Ag NPs with the investigation of their antioxidant and antimicrobial activities. *J Mol Liq.* 2017;248: 1044–1049.
- Human JP. Breeding blush pears (*Pyrus communis* L.) in South Africa. *Acta Hort.* 2013;976:383–388.
- Ghodake G, Lee DS. Green synthesis of gold nanostructures using pear extract as effective reducing and coordinating agent. *Korean J Chem Eng.* 2011;28(12):2329–2335.
- Huang JT, Yang XX, Zeng QL, et al. A simple green route to prepare stable silver nanoparticles with pear juice and a new selective colorimetric method for detection of cysteine. *Analyst.* 2013; 138(18):5296–5302.
- Ghodake G, Eom CY, Kim SW, et al. Biogenic nano-synthesis; towards the efficient production of the biocompatible gold nanoparticles. *Bull Korean Chem Soc.* 2010;31(10):2771–2775.
- Qureyshi S, Niazi KUK, Usman M. Silver nanoparticles mediated through green route using pyrus seed extract. *J. Basic. Appl. Chem.* 2016;6(1):1–7.
- Hudina M, Štampar F. Sugars and organic acids contents of European (*Pyrus communis* L.) and Asian (*Pyrus serotina* reh.) pear cultivars. *Acta Aliment.* 2000;29(3):217–230.
- Dube P, Meyer S, Marnewick JL. Antimicrobial and antioxidant activities of different solvent extracts from fermented and green honeybush (*Cyclopia intermedia*) plant material. *South African J Bot.* 2017;110:184–193.
- Dubois M, Gilles K, Hamilton JK, et al. A colorimetric method for the determination of sugars. *Nature.* 1951;168(4265):167.
- Dube P, Meyer S, Madiehe A, et al. Antibacterial activity of biogenic silver and gold nanoparticles synthesized from *Salvia africana-lutea* and *Sutherlandia frutescens*. *Nanotechnology.* 2020; 31(50):505607.
- Sibuyi NRS, Thihe VC, Panjtan-Amiri K, et al. Green synthesis of gold nanoparticles using acai berry and elderberry extracts and investigation of their effect on prostate and pancreatic cancer cells. *Nanobiomedicine.* 2021;8:1849543521995310.

- [28] Khodadadi B, Bordbar M, Yeganeh-Faal A, et al. Green synthesis of Ag nanoparticles/clinoptilolite using vaccinium macrocarpon fruit extract and its excellent catalytic activity for reduction of organic dyes. *J Alloys* 2017;719:82–88.
- [29] Taha ZK, Hawar SN, Sulaiman GM. Extracellular biosynthesis of silver nanoparticles from *Penicillium italicum* and its antioxidant, antimicrobial and cytotoxicity activities. *Biotechnol Lett.* 2019; 41(8–9):899–914.
- [30] Kumar H, Bhardwaj K, Dhanjal DS, et al. Fruit extract mediated green synthesis of metallic nanoparticles: a new avenue in pomology applications. *Int J Mol Sci.* 2020;21:1–18.
- [31] Li D, Liu Z, Yuan Y, et al. Green synthesis of gallic acid-coated silver nanoparticles with high antimicrobial activity and low cytotoxicity to normal cells. *Process Biochem.* 2015;50(3):357–366.
- [32] Bouqellah NA, Mohamed MM, Ibrahim Y. Synthesis of eco-friendly silver nanoparticles using *Allium sp.* and their antimicrobial potential on selected vaginal bacteria. *Saudi J Biol Sci.* 2019;26(7): 1789–1794.
- [33] Li X, Wang T, Zhou B, et al. Chemical composition and antioxidant and anti-inflammatory potential of peels and flesh from 10 different pear varieties (*Pyrus spp.*). *Food Chem.* 2014;152:531–538.
- [34] Mat Yusuf SNA, Che Mood CNA, Ahmad NH, et al. Optimization of biogenic synthesis of silver nanoparticles from flavonoid-rich *Clinacanthus nutans* leaf and stem aqueous extracts: biogenic synthesis of *C. nutans* AgNPs. *R Soc Open Sci.* 2020;7(7):200065.
- [35] Choi Y, Choi MJ, Cha SH, et al. Catechin-capped gold nanoparticles: green synthesis, characterization, and catalytic activity toward 4-nitrophenol reduction. *Nanoscale Res Lett.* 2014;9:1–8.
- [36] Fafal T, Taştan P, Tüzün BS, et al. Synthesis, characterization and studies on antioxidant activity of silver nanoparticles using *Asphodelus aestivus* brot. aerial part extract. *South African J Bot.* 2017;112:346–353.
- [37] Alegria ECBA, Ribeiro APC, Mendes M, et al. Effect of phenolic compounds on the synthesis of gold nanoparticles and its catalytic activity in the reduction of nitro compounds. *Nanomaterials.* 2018;8:320.
- [38] Firoozi S, Jamzad M, Yari M. Biologically synthesized silver nanoparticles by aqueous extract of *Satureja intermedia* C.A. Mey and the evaluation of total phenolic and flavonoid contents and antioxidant activity. *J Nanostruct Chem.* 2016;6(4):357–364.
- [39] Katti KK, Kattumuri V, Bhaskaran S, et al. Facile and general method for synthesis of sugar-coated gold nanoparticles. *Int J Nanotechnol: Biomed.* 2009;1(1):1–8.
- [40] Singh R, Wagh P, Wadhvani S, et al. Synthesis, optimization, and characterization of silver nanoparticles from *Acinetobacter calcoaceticus* and their enhanced antibacterial activity when combined with antibiotics. *Int J Nanomedicine.* 2013;8:4277–4290.
- [41] Sherry LJ, Jin R, Mirkin CA, et al. Localized surface plasmon resonance spectroscopy of single silver triangular nanoprisms. *Nano Lett.* 2006;6(9):2060–2065.
- [42] Edison TJI, Sethuraman MG. Biogenic robust synthesis of silver nanoparticles using punica granatum peel and its application as a green catalyst for the reduction of an anthropogenic pollutant 4-nitrophenol. *Spectrochim Acta A Mol Biomol Spectrosc.* 2013; 104:262–264.
- [43] Velgosová O, Mražíková A, Marcinčáková R. Influence of pH on green synthesis of Ag nanoparticles. *Mater Lett.* 2016;180: 336–339.
- [44] Luo L, Chen Y, Zhang L, et al. SERS assay for pyrophosphate based on its competitive binding to Cu(II) ion on silver nanoparticles modified with cysteine and rhodamine 6G. *Microchim Acta.* 2017;184(2):595–601.
- [45] Indana MK, Gangapuram BR, Dadigala R, et al. A novel green synthesis and characterization of silver nanoparticles using gum tragacanth and evaluation of their potential catalytic reduction activities with methylene blue and Congo red dyes. *J Anal Sci Technol.* 2016;7:1–9.
- [46] Kredy HM. The effect of pH, temperature on the green synthesis and biochemical activities of silver nanoparticles from *Lawsonia inermis* extract. *J Pharm Sci Res.* 2018;10:2022–2026.
- [47] Alqadi MK, Abo Noqta OA, Alzoubi FY, et al. PH effect on the aggregation of silver nanoparticles synthesized by chemical reduction. *Mater Sci-Pol.* 2014;32(1):107–111.
- [48] Zada S, Ahmad A, Khan S, et al. Biogenic synthesis of silver nanoparticles using extracts of leptolyngbya JSC-1 that induce apoptosis in HeLa cell line and exterminate pathogenic bacteria. *Artif Cells Nanomed Biotechnol.* 2018;46(3):S471–S480.
- [49] Krishnaraj C, Jagan EG, Rajasekar S, et al. Synthesis of silver nanoparticles using *acalypha indica* leaf extracts and its antibacterial activity against water borne pathogens. *Colloids Surf B Biointerfaces.* 2010;76(1):50–56.
- [50] Banala RR, Nagati VB, Karnati PR. Green synthesis and characterization of carica papaya leaf extract coated silver nanoparticles through X-ray diffraction, electron microscopy and evaluation of bactericidal properties. *Saudi J Biol Sci.* 2015;22(5):637–644.
- [51] Adedayo AI, Oyeyemi AD, Ramatu A, et al. Biosynthesis of silver nanoparticles using aqueous extract of buchholzia coriacea (wonderful kola) seeds and their antimicrobial activities. *Ann Food Sci Technol.* 2017;18:671–679.
- [52] Masum MI, Siddiq MM, Ali KA, et al. Biogenic synthesis of silver nanoparticles using *Phyllanthus emblica* fruit extract and its inhibitory action against the pathogen *Acidovorax oryzae* strain RS-2 of rice bacterial brown stripe. *Front Microbiol.* 2019;10:818–820.
- [53] Ryu AH, Eckalbar WL, Kreimer A, et al. Use antibiotics in cell culture with caution: genome-wide identification of antibiotic-induced changes in gene expression and regulation. *Sci Rep.* 2017;7:1–9.
- [54] Lategan K, Alghadi H, Bayati M, et al. Effects of graphene oxide nanoparticles on the immune system biomarkers produced by RAW 264.7 and human whole blood cell cultures. *Nanomaterials.* 2018;8:125.